November, 1988] © *1988 The Chemical Society of Japan* *Bull. Chem. Soc. Jpn.*, *61*, 3869—3875 (1988)

Structure of Mixed Ligand Complex [Cu(pan)(phen)]BF$_4$ with Special Reference to the Acceleration of the Ligand Substitution Reaction

Hiroko WADA,* Motoo SHIRO,† Akio YUCHI, and Genkichi NAKAGAWA
Department of Applied Chemistry, Nagoya Institute of Technology,
Gokiso-cho, Showa-ku, Nagoya 466
†Shionogi Research Laboratories, Shionogi & Co., Ltd., Fukushima-ku, Osaka 553

(Received March 22, 1988)

The crystal structures of [1-(2-pyridylazo)-2-naphtholato]copper(II) complexes, [Cu(pan)(phen)]BF$_4$ as well as [Cu(pan)(H$_2$O)]ClO$_4$ and [Cu$_2$(pan)$_2$(H$_2$O)$_3$](BF$_4$)$_2$ have been determined. In these complexes pan$^-$ anion coordinates with copper(II) as a tridentate ligand and all complexes have square pyramidal geometry. In the mixed ligand complex [(Cu(pan)(phen)]BF$_4$, 1,10-phenanthroline occupies the forth position in the basal plane and the apical site, thus the structure is fairly distorted. This distorted structure is responsible for the fast substitution of [Cu(pan)(phen)]$^+$ complex with edta^{4-}.

In the series of studies on the ligand substitution reaction, Tanaka and his coworkers found that the reactivity of the complexes can be quantitatively accounted for by the electron donation from the ligand already bound to the metal ion.[1)]

In our previous works,[2–4)] it was found that the color change of 1-(2-pyridylazo)-2-naphthol (PAN, Hpan) or Xylenol Orange indicator in chelatometric titration of copper(II) with ethylenediamine-*N,N,N′,N′*-tetraacetic acid (EDTA, H$_4$edta) is accelerated by the addition of a small amount of bidentate ligand such as 1,10-phenanthroline (phen), 2,2′-bipyridine, 8-quinolinol, sodium diethyldithiocarbamate. The rate and mechanism of substitution reaction of [Cu(pan)]$^+$ complex with EDTA had been studied in detail.[3)] In the absence of phen, the ligand substitution reaction with EDTA proceeds as

$$\begin{aligned}&\mathrm{Cu(pan)^+ + edta' \rightleftharpoons Cu(pan)(edta)}\\&\qquad\longrightarrow \mathrm{Cu(edta)^{2-} + Hpan}\end{aligned}\qquad(1)$$

The rate depends on the total concentration of EDTA not combined with copper(II), [edta′], and the rate constant is; $k=1.7\times10^3\,\mathrm{dm^3\,mol^{-1}\,s^{-1}}$, whereas in the presence of phen, the rate does not depend on the concentration of edta′, but depends mainly on the concentration of hydrogen ion. The mechanism of the substitution reaction is expressed as

$$\begin{aligned}&\mathrm{[Cu(pan)(phen)]^+ + H^+}\\&\qquad\longrightarrow \mathrm{Cu(phen)^{2+} + Hpan}\qquad(2)\\&\mathrm{Cu(phen)^{2+} + edta' \rightleftharpoons Cu(edta)^{2-} + phen}\end{aligned}$$

The rate constant is; $k=1.6\times10^6\,\mathrm{dm^3\,mol^{-1}\,s^{-1}}$. The faster substitution Reaction (2) compared with Reaction (1) is attributed to the distorted structure of the mixed ligand complex [Cu(pan)(phen)]$^+$. Also the formation of the mixed ligand complex of [Cu(pan)]$^+$ with some other bidentate ligands such as 2,2′-bipyridine, bathophenanthroline, 8-quinolinol, diethyldithiocarbamate, etc. was found, and the stability constants of these mixed ligand complexes were determined spectrophotometrically.[5)]

In this work the crystal structure of [Cu(pan)(phen)]BF$_4$ (**1**) was determined as well as [Cu(pan)(H$_2$O)]ClO$_4$ (**2**), [Cu$_2$(pan)$_2$(H$_2$O)$_3$](BF$_4$)$_2$ (**3**) for comparison. Although crystal structure of complex **2** had been determined previously by Ooi et al.,[6)] the refined geometry as well as the other complexes was determined. The influence of phen on the acceleration of the substitution reaction is discussed by comparing the bond lengths of Cu–pan in the complex **1** with those in the complexes **2**, **3**, and [Cu(pan)Cl] (**4**).[7)]

Experimental

Preparation of the Complexes. [Cu(pan)(phen)]BF$_4$(**1**) was prepared by adding an ethanol solution of equal concentration of Hpan and phen to an aqueous solution of Cu(BF$_4$)$_2$ in the molar ratio of 1 : 1. After slow evaporation of the solvent at room temperature, dark green crystals with metallic luster were obtained together with orange ones of Hpan. The results of elemental analysis of the dark green crystal: C, 55.9%; H, 2.9%; N, 12.1%, Calcd for [Cu(pan)(phen)]BF$_4$: C, 56.0%; H, 3.1%; N, 12.1%. [Cu(pan)(H$_2$O)]ClO$_4$ (**2**) was prepared from Hpan and Cu(ClO$_4$)$_2$ and [Cu$_2$(pan)$_2$(H$_2$O)$_3$](BF$_4$)$_2$ (**3**) from Hpan and Cu(BF$_4$)$_2$ in the similar way. All crystals have similar color as [Cu(pan)(phen)]BF$_4$.

X-Ray Analysis. Crystallographic details for **1**, **2**, and **3** are listed in Table 1. The unit cell parameters were determined by least-squares fitting of 2θ values of 20 reflections ($0.20<\sin\theta/\lambda<0.24$ Å^{-1}) measured on a Rigaku AFC-5 diffractometer equipped with a graphite monochromator.

Three-dimensional intensity data were collected by ω–2θ scan technique using Cu $K\alpha$ radiation (λ=1.54178 Å) for **1** and using Mo $K\alpha$ radiation (λ=0.71069 Å) for **2** and **3**. Three standard reflections monitored every 100 reflections showed no significant change during the data collection. All intensities were corrected for Lorentz and polarization factors, but not for absorption effects.

The structures were solved by the conventional heavy atom method, and improved by block-diagonal least-squares refinement of the positional and the thermal parameters of the non-H atoms and the positional ones of the H atoms

Table 1. Crystallographic Details for **1**, **2**, and **3**

Complex	**1**	**2**	**3**
Formula	$[Cu(pan)(phen)]BF_4$	$[Cu(pan)(H_2O)]ClO_4$	$[Cu(pan)(H_2O)](BF_4)$ $\cdot[Cu(pan)(H_2O)_2]BF_4$
Formula weight	578.8	429.3	851.3
Crystal system	Triclinic	Triclinic	Triclinic
Space group	$P\bar{1}$	$P\bar{1}$	$P\bar{1}$
a/Å	11.945(1)	9.342(7)[a]	11.095(5)
b/Å	13.630(3)	10.356(5)	20.367(5)
c/Å	7.651(2)	8.208(5)	7.539(2)
α/°	103.63(3)	93.31(5)	96.13(2)
β/°	92.09(3)	95.01(6)	102.14(2)
γ/°	84.43(2)	83.33(5)	80.98(3)
V/Å^3	1204.7(6)	784.8(8)	1640(1)
Z	2	2	2
D_c/g cm^{-3}	1.596	1.817	1.724
μ/cm^{-1}	18.9 (Cu $K\alpha$)	16.6 (Mo $K\alpha$)	14.5 (Mo $K\alpha$)
Crystal size/mm	0.3×0.1×0.1	0.3×0.15×0.1	0.4×0.15×0.05
$\sin\theta_{max}\cdot\lambda^{-1}$/Å^{-1}	0.588	0.595	0.595
Number of unique reflections	4092	2761	5761
Number of observed reflections [$\lvert F_o\rvert>2\sigma(F_o)$]	3708	2424	4652
Number of reflections used for least-squares refinement	3586	2417	4625
R	0.054	0.040	0.045
R_w	0.079	0.053	0.060
S	1.164	0.938	1.170

a) The unit cell parameters described in Ref. 6 are as follows: a=10.38, b=8.22, c=9.35 Å, α=85°20′, β=96°48′, γ=93°19′.

which were located on difference electron density maps. The temperature factor of each H atom was assumed to be isotropic and equal to the equivalent isotropic temperature factor of the attached atom. The function minimized in the refinement was $\sum(w|\Delta F|^2)$. The weighting scheme was $w=[\sigma^2(F_o)+c^2|F_o|^2]^{-1}$ for observed reflections with $w^{1/2}|\Delta F|<4$ and $w=0$ otherwise. The values of c^2 were 0.00381, 0.00231, and 0.00144 for **1**, **2**, and **3**, respectively. The parameter shifts in the final cycle were less than half the corresponding σ values. The atomic scattering factors were calculated using the analytical expression $f=\sum[a_i\exp(-b_i\sin^2\theta/\lambda^2)]+c$ (i=1—4).[8] Computations using the programs of MULTAN84, PLUTO, and XPACK86 SHIONOGI were performed by a FACOM M-340R computer at Shionogi Research Laboratories.

Structural Description

Perspective views of **1** and **2** are shown in Figs. 1 and 2, respectively. In the crystal of **3**, the two complexes which should be differently described as $[Cu(pan)(H_2O)]BF_4$ (**3A**) and $[Cu(pan)(H_2O)_2]BF_4$ (**3B**) are included (Figs. 3 and 4). All the complexes have the same type of coordination geometry around Cu(II): square pyramidal geometry or square planar one with weak interaction between Cu and the atom at the position corresponding to the apex. Three corners of the basal plane are occupied by the atoms of pyridyl N, azo N adjacent to the naphthol group and naphthol O of the pan$^-$ ligand. The atoms at the fourth corner of the plane (X) and the apical position (Y) are shown in Fig. 5 along with the atom-numbering systems of the

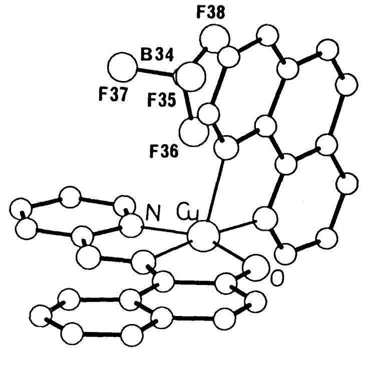

Fig. 1. Perspective drawing of **1** with atomic numbering system for BF_4^-.

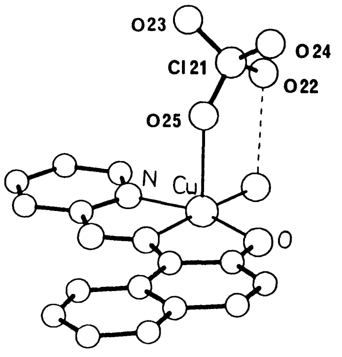

Fig. 2. Perspective drawing of **2** with atomic numbering system for ClO_4^-. Broken line represents the intramolecular hydrogen bond of O(20)···O(22).

phen and pan$^-$ ligands. The square pyramid of **1**, in which the axial Cu-N bond is considerably tilted to the basal plane [∠N(20)-Cu-N(29)=79.4(1)°], is the most distorted in those of the complexes.

Atomic coordinates and equivalent isotropic temperature factors are listed in Table 2. The bond lengths and angles involving Cu, and the deviations of Cu from the basal plane are given in Table 3, where those of [Cu(pan)Cl] (**4**)[7] are listed together for comparison. The less planarity of the basal plane in **3A** and **3B**, judged based on the rms deviation of the constituent atoms from the plane, may be mainly caused by that of the pan$^-$ ligand as described later.

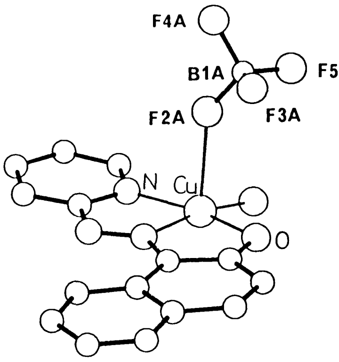

Fig. 3. Perspective drawing of **3A** with atomic numbering system for BF_4^-.

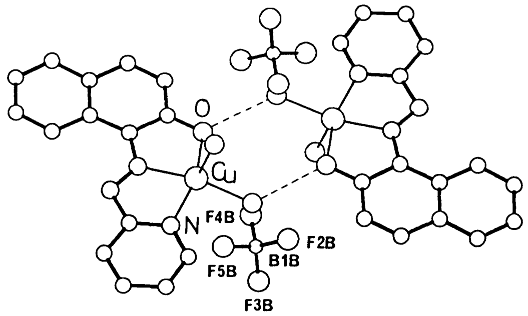

Fig. 4. Perspective drawing of **3B** with atomic numbering system for BF_4^-. Broken lines represent the intermolecular hydrogen bonds of O(19)···O(20).

The bond length of Cu-N(20) in **1** is compatible with the equatorial Cu-N bonds in [Cu(gg)(phen)]-$3H_2O$,[9] 2.009(5) Å, and in [$Cu(phen)_3$]$(ClO_4)_2$,[10] 2.00(1) and 2.02(1) Å (gg=glycylglycine dianion). However, the bond of Cu-N(29) in **1** is shorter than the axial Cu-N bonds, 2.275(5) Å in [Cu(gg)(phen)]-$3H_2O$ and 2.34(1) and 2.32(1) Å in [$Cu(phen)_3$]$(ClO_4)_2$, indicating the N(29) atom to be tightly bound to Cu.

For **2**, **3A**, and **3B** (X=H_2O), the deviation of Cu from the basal plane increases as the distance between Cu and the apical atom decreases. The bonds of Cu-N(1), Cu-N(8), Cu-O(19), and Cu-O(20), according to usual statistical tests, are respectively lengthened in the order of [**2**, **3A**]<**3B**, **2**<[**3A**, **3B**], **3A**<[**2**, **3B**], and [**2**, **3A**]<**3B**, though differences among those in [ ] are not significant. This suggests that the equatorial bonds tend to be weakened with shortening the interatomic distance between Cu and Y. The bonds in **1**, except Cu-N(8), are significantly longer than the corresponding ones in **3B**, a similar tendency having been pointed out on comparison between [Cu(gg)(phen)]$3H_2O$ and [$Cu(gg)(H_2O)_2$]-H_2O.[9]

In the crystal of **4**, the centrosymmetric binuclear complex molecule, [$Cu(pan)Cl]_2$, bridged through two Cl atoms is formed: each Cl atom lies at the basal plane of one square pyramid and at the apex of another one. The bond lengths of Cu-pan$^-$ are very similar to the corresponding one in **1**.

The bond lengths and angles of the phen and pan$^-$ ligands are normal and agree well within experimental errors with those in the respective free ligands. The phen ligand in **1** is bowed along its longest molecular axis, the dihedral angle between the two C_5N rings being 4.3°. For pan$^-$ ligand, the rms deviations of the constituent atoms from the mean plane are 0.016, 0.030, 0.055, 0.040, and 0.016 Å for **1**, **2**, **3A**, **3B**, and **4**, respectively. The less planarity of the ligand observed in **3A** and **3B** is mainly caused by the twist between the pyridine and naphthol rings: the

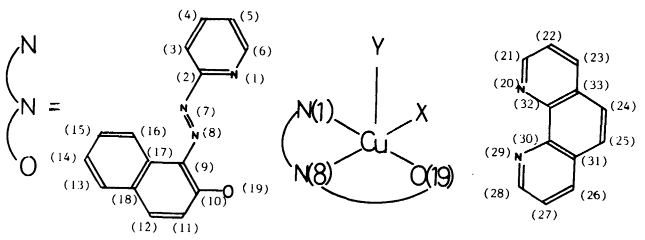

	1	2	3A	3B	4
X	phen[N(20)]	H_2O[O(20)]	H_2O[O(20A)]	H_2O[O(20B)]	Cl
Y	phen[N(29)]	ClO_4[O(25)]	BF_4[F(2A)]	H_2O[O(21B)]	Cl

Fig. 5. Coordination geometry of the compexes and atomic numbering systems of pan$^-$ and phen ligands.

Table 2. Atomic Coordinates ($\times 10^4$) and Equivalent Isotropic Temperature Factors ($Å^2 \times 10^2$) with Estimated Standard Deviations in Parentheses for **1**, **2**, and **3**

1	*x*	*y*	*z*	B_{eq}
Cu	7761.6(3)	3557.3(3)	1282.6(5)	408(1)
N(1)	9030(2)	2601(2)	1846(3)	327(6)
C(2)	9955(2)	3089(2)	2419(4)	316(7)
C(3)	10923(3)	2601(2)	3003(5)	409(9)
C(4)	10938(3)	1589(3)	2983(5)	480(11)
C(5)	9996(3)	1095(3)	2406(6)	508(12)
C(6)	9063(3)	1616(2)	1836(5)	441(10)
N(7)	9941(2)	4117(2)	2426(3)	312(6)
N(8)	8980(2)	4444(2)	1834(3)	297(6)
C(9)	8717(2)	5403(2)	1651(3)	306(7)
C(10)	7599(2)	5504(2)	908(4)	358(8)
C(11)	7157(3)	6470(2)	648(5)	419(9)
C(12)	7791(3)	7271(2)	1055(4)	385(9)
C(13)	9522(3)	8043(2)	2211(4)	382(9)
C(14)	10581(3)	7993(2)	2941(5)	407(9)
C(15)	11070(2)	7069(2)	3226(4)	388(9)
C(16)	10491(2)	6215(2)	2800(4)	328(7)
C(17)	9394(2)	6251(2)	2081(3)	289(7)
C(18)	8910(2)	7183(2)	1784(4)	315(7)
O(19)	6994(2)	4743(2)	501(3)	446(7)
N(20)	6586(2)	2583(2)	407(3)	305(6)
C(21)	6505(3)	1989(2)	−1230(4)	388(9)
C(22)	5685(3)	1309(3)	−1715(5)	454(10)
C(23)	4933(3)	1245(2)	−462(5)	455(10)
C(24)	4226(3)	1828(4)	2678(7)	669(16)
C(25)	4285(4)	2459(5)	4298(7)	731(18)
C(26)	5193(5)	3901(5)	6367(5)	935(23)
C(27)	6003(5)	4547(4)	6631(5)	885(20)
C(28)	6764(4)	4511(3)	5268(5)	670(14)
N(29)	6714(2)	3842(2)	3686(3)	431(8)
C(30)	5894(3)	3207(2)	3407(4)	408(9)
C(31)	5102(4)	3177(4)	4703(5)	622(14)
C(32)	5827(2)	2531(2)	1659(4)	320(7)
C(33)	4995(2)	1860(2)	1278(5)	412(9)
B(34)	7185(3)	231(3)	3858(5)	430(11)
F(35)	6989(3)	1277(2)	4436(4)	728(10)
F(36)	7380(2)	−47(2)	2025(3)	567(8)
F(37)	8201(3)	13(2)	4707(5)	921(13)
F(38)	6372(4)	−275(4)	4223(5)	1514(25)

2	*x*	*y*	*z*	B_{eq}
Cu	2904.4(3)	1764.3(3)	4929.2(4)	235(1)
N(1)	1943(3)	3233(2)	6212(3)	250(6)
C(2)	484(3)	3316(3)	5933(3)	238(9)
C(3)	−426(3)	4259(3)	6698(4)	300(10)
C(4)	191(4)	5154(3)	7783(4)	354(11)
C(5)	1680(4)	5066(3)	8086(4)	391(12)
C(6)	2524(4)	4098(3)	7273(4)	331(11)
N(7)	−110(2)	2383(2)	4828(3)	237(7)
N(8)	896(2)	1566(2)	4273(3)	206(7)
C(9)	677(3)	538(3)	3208(3)	218(8)
C(10)	2027(3)	−202(3)	2884(3)	236(9)
C(11)	2028(3)	−1309(3)	1779(4)	286(10)
C(12)	765(3)	−1662(3)	1074(4)	278(9)
C(13)	−1892(4)	−1410(3)	653(4)	314(10)
C(14)	−3226(4)	−762(4)	997(4)	344(11)
C(15)	−3293(3)	339(4)	2049(4)	340(11)
C(16)	−2050(3)	812(3)	2772(4)	271(9)
C(17)	−682(3)	148(3)	2473(3)	232(9)
C(18)	−615(3)	−966(3)	1393(3)	255(9)
O(19)	3234(2)	139(2)	3606(3)	275(7)
O(20)	4882(2)	1939(2)	5772(3)	317(7)
Cl(21)	4322(1)	3845(1)	2329(1)	341(3)
O(22)	5519(3)	3622(3)	3551(4)	528(11)

Table 2. (Continued)

2	x	y	z	B_{eq}
O(23)	3837(3)	5189(3)	2304(5)	620(12)
O(24)	4789(4)	3379(4)	777(4)	704(15)
O(25)	3163(3)	3133(3)	2717(3)	475(10)

3	x	y	z	B_{eq}
Cu(1A)	5775.2(4)	3747.3(2)	5096.7(6)	278(1)
N(1A)	5520(3)	2850(1)	5563(4)	290(9)
C(2A)	6479(3)	2384(2)	5216(4)	277(11)
C(3A)	6498(4)	1715(2)	5417(5)	333(12)
C(4A)	5489(4)	1518(2)	5916(5)	390(13)
C(5A)	4499(4)	1993(2)	6260(5)	386(13)
C(6A)	4558(4)	2655(2)	6075(5)	345(12)
N(7A)	7479(3)	2591(1)	4656(4)	283(9)
N(8A)	7288(3)	3228(1)	4508(4)	256(9)
C(9A)	8074(3)	3591(2)	4041(4)	268(10)
C(10A)	7556(3)	4278(2)	4018(5)	288(11)
C(11A)	8252(4)	4739(2)	3547(5)	354(12)
C(12A)	9394(4)	4527(2)	3182(6)	371(13)
C(13A)	11184(4)	3663(2)	2955(5)	397(14)
C(14A)	11734(4)	3016(2)	3032(6)	420(14)
C(15A)	11095(4)	2529(2)	3432(6)	420(14)
C(16A)	9899(4)	2703(2)	3759(5)	344(12)
C(17A)	9311(3)	3358(2)	3685(4)	267(10)
C(18A)	9973(3)	3848(2)	3276(5)	325(12)
O(19A)	6475(2)	4479(1)	4431(4)	333(8)
O(20A)	4474(3)	4263(1)	6205(4)	386(9)
B(1A)	3876(5)	3941(3)	622(7)	419(16)
F(2A)	4475(3)	3616(2)	2122(4)	744(13)
F(3A)	4728(3)	4130(2)	−210(5)	924(17)
F(4A)	3214(4)	3490(2)	−527(5)	925(17)
F(5A)	3115(5)	4442(2)	1112(8)	1420(26)
Cu(1B)	8213.9(4)	897.2(2)	10255.6(7)	337(1)
N(1B)	6504(3)	1058(1)	10774(4)	316(10)
C(2B)	6013(3)	1706(2)	10651(5)	292(11)
C(3B)	4820(3)	1939(2)	10926(5)	342(12)
C(4B)	4134(4)	1492(2)	11399(5)	385(13)
C(5B)	4665(4)	836(2)	11597(6)	410(14)
C(6B)	5842(4)	638(2)	11254(6)	382(13)
N(7B)	6721(3)	2151(1)	10173(4)	299(9)
N(8B)	7776(3)	1844(2)	9897(4)	294(9)
C(9B)	8653(3)	2135(2)	9369(5)	283(11)
C(10B)	9691(3)	1639(2)	9107(5)	332(12)
C(11B)	10727(4)	1849(2)	8578(6)	407(14)
C(12B)	10729(4)	2497(2)	8381(6)	407(14)
C(13B)	9752(4)	3674(2)	8388(5)	397(14)
C(14B)	8764(4)	4153(2)	8600(5)	417(14)
C(15B)	7703(4)	3977(2)	9069(5)	363(13)
C(16B)	7633(3)	3329(2)	9316(5)	316(12)
C(17B)	8639(3)	2824(2)	9120(4)	290(11)
C(18B)	9704(4)	3003(2)	8614(5)	346(13)
O(19B)	9682(3)	1017(1)	9344(4)	438(10)
O(20B)	8324(3)	−89(1)	9807(5)	484(10)
O(21B)	9163(3)	838(2)	13103(5)	612(13)
B(1B)	7569(5)	−438(3)	5010(9)	514(19)
F(2B)	8093(4)	−872(2)	6290(6)	962(17)
F(3B)	6759(4)	−676(2)	3622(6)	1175(22)
F(4B)	8424(5)	−210(3)	4366(7)	1497(30)
F(5B)	7046(6)	75(3)	5903(8)	1608(33)

dihedral angles between the two rings are 1.4, 1.9, 4.5, 3.9, and 1.2° in the above order.

The atom-numbering systems of the BF$_4^-$ and ClO$_4^-$ anions are presented in Figs. 1—4. The bond lengths of B–F average 1.37 Å for **1**, 1.35 Å for **3A** and 1.33 Å for **3B**, and those of Cl–O average 1.43 Å for **2**. The mean bond angles of F–B–F are all 109° for **1**, **3A**, and **3B**, and that of O–Cl–O is 110° for **2**. The temperature

Table 3. Geometries of the Complexes of **1**, **2**, **3A**, **3B**, and **4** (Standard Deviations in Parentheses)

Complex	**1**	**2**	**3A**	**3B**	**4**
(a) Bond length/Å					
Cu-N(1)	2.003(3)	1.973(3)	1.971(3)	1.987(3)	1.991(2)
Cu-N(8)	1.953(3)	1.937(2)	1.947(3)	1.947(4)	1.964(2)
Cu-O(19)	1.985(3)	1.958(2)	1.940(3)	1.954(3)	1.984(2)
Cu-X	2.015(3)	1.940(2)	1.931(3)	1.990(4)	2.263(1)
Cu-Y	2.199(3)	2.412(2)	2.411(4)	2.190(4)	2.647(1)
(b) Bond angles/°					
N(1)-Cu-N(8)	78.7(1)	79.7(1)	79.9(1)	79.4(2)	78.53(9)
N(1)-Cu-O(19)	158.5(1)	161.6(1)	162.7(1)	160.6(1)	159.3
N(1)-Cu-X	100.2(1)	98.0(1)	98.6(1)	96.8(1)	97.36(7)
N(1)-Cu-Y	102.5(1)	92.0(1)	89.0(1)	95.4(1)	91.26(7)
N(8)-Cu-O(19)	81.9(1)	82.7(1)	82.7(1)	82.3(2)	81.50(9)
N(8)-Cu-Y	172.9(1)	175.2(1)	167.8(1)	161.2(2)	170.0
N(8)-Cu-Y	107.8(1)	94.2(1)	97.1(1)	105.8(2)	96.90(7)
O(19)-Cu-X	97.8(1)	99.2(1)	98.4(1)	98.5(1)	101.50(7)
O(19)-Cu-Y	92.2(1)	94.3(1)	92.5(1)	95.7(1)	96.34(7)
X-Cu-Y	79.4(1)	90.0(1)	94.9(1)	92.8(2)	92.21(3)
Cu-N(1)-C(2)	111.2(2)	111.6(2)	111.2(3)	111.1(3)	112.2
Cu-N(1)-C(6)	130.4(2)	129.5(2)	129.6(3)	129.9(3)	129.5
Cu-N(8)-N(7)	120.1(2)	120.0(2)	119.3(3)	119.9(3)	120.1
Cu-N(8)-C(9)	115.4(2)	115.0(2)	114.5(3)	115.5(3)	115.3
Cu-O(19)-C(10)	110.6(2)	111.3(2)	111.3(3)	111.5(3)	111.4
Cu-N(20)-C(21)	126.4(2)				
Cu-N(20)-C(32)	115.2(2)				
Cu-N(29)-C(28)	131.4(3)				
Cu-N(29)-C(30)	110.1(2)				
(c) Deviations of Cu from the basal plane towards the apex/Å					
	0.152(1)	0.084(1)	0.109(1)	0.228(1)	0.145
(d) Deviations of the equatorial donor atoms from the basal plane and their rms values in parentheses/Å					
	−0.029	−0.015	−0.109	−0.113	−0.036
	ca. 0.034	ca. 0.013	ca. 0.096	ca. 0.066	ca. 0.030
	(0.029)	(0.012)	(0.092)	(0.081)	(0.026)

factors of the atoms of the anions are larger than those of the constituent atoms of the pan$^-$ and phen ligands, some of which exhibit a large anisotropy. The H atoms of all the complexes lie at the positions not far from those expected on chemical grounds.

In **2** and **3**, the two complexes related by an inversion center are linked to form a binuclear unit by the hydrogen bonds between O(19) and O(20) individually lying on different basal planes of the two square pyramids: the interatomic distances are 2.661(3), 2.666(4), and 2.688(5) Å for **2**, **3A**, and **3B**, respectively. This is represented for **3B** in Fig. 4. The basal planes of the two complexes, parallel to each other, are differently separated in each binuclear unit probably subjected to different packing effects: the distances are respectively 1.40, 0.61, and 1.14 Å for **2**, **3A**, and **3B**. The above-mentioned dihedral angle between the pyridine and naphthol rings in the pan$^-$ ligand increases with decreasing distance in the order of **2**>**3B**>**3A**. Smaller angles are observed for **1** and **4** in which such hydrogen bonds are not formed. Therefore, we assumed that the distortion in the pan$^-$ ligand may be caused by the formation of the intermolecular hydrogen bonds in the binuclear unit. The O(20) atom forms a hydrogen bonds with O(22) [2.741(4) Å] in **2** and a bifurcated one with F(2B) and F(5B) [2.929(4) and 3.015(4) Å] in **3B**.

Discussion

The bond lengths of Cu–pan in the mixed complex **1** were similar to those in complex **4**. However, the mixed ligand phen complex **1** is expected to have the same structure in aqueous solution, whereas in the mixed ligand chloro complex **4** Cl$^-$ at apical position should be replaced with water molecule. The resulted complex may have the structure close to complex **3B**, because the interaction with inert anions at apical site is weak even in solid as shown in complexes **2** and **3A**.

In the ligand substitution reaction of the mixed ligand complex [Cu(pan)(phen)]$^+$ with multidentate ligand such as edta^{4-}, the reaction mechanism is different from that of the unidentate mixed ligand complex. The mixed ligand complex with the unidentate ligand has at least one water molecule in X or Y position. The water molecule is labile and easily displaced by a moiety of the entering ligand before or in the rate-determining step. Thus the rate is propotional to the concentration of the entering ligand. The reaction is accelerated by the presence of unidentate ligand (L), because the bonds between Cu(II) and pan^- are weakened depending on the electron donation from L to Cu(II).

On the other hand, a bidentate ligand such as phen occupies not only the basal site but also the apical one, then there left no site for the entering ligand to attack, but Cu–pan bonds are weakened by the coordination of phen as seen from the results of the X-ray analysis. This is also found from the decreased stability constant of $[Cu(pan)(phen)]^+$ compared with that of $[Cu(pan)]^+$: $\log K^{\mathrm{pan}}_{\mathrm{Cu(pan)(phen)}}=12.20$ and $\log K^{\mathrm{pan}}_{\mathrm{Cu(pan)}}=15.58$ (5%dioxane, 0.1 mol dm^{-3} KNO_3 at 25 °C). Therefore, the Cu–pan bond in the mixed ligand complex **1** is easily broken by the attack of proton (rate-determining step). The rate of the reaction does not depend on the concentration of the entering ligand but depends on the concentration of hydrogen ion. The resulted $[Cu(phen)]^{2+}$ complex is rapidly replaced with $edta^{4-}$. As the rate constant of Reaction (2) is much larger than that of Reaction (1), the rate of the color change of PAN indicator is accelerated by the addition of phen in the chelatometric titration of copper(II).

References

1) M. Tabata and M. Tanaka, *Inorg. Chem.*, **17**, 2779 (1978) and the references cited therein.

2) G. Nakagawa and H. Wada, *Talanta*, **20**, 829 (1973).

3) G. Nakagawa and H. Wada, *Talanta*, **22**, 563 (1975).

4) H. Wada, T. Ishizuki, and G. Nakagawa, *Bull. Chem. Soc. Jpn.*, **50**, 2104 (1977).

5) H. Wada, K. Ikuta, and G. Nakagawa, *Bull. Chem. Soc. Jpn.*, **51**, 2916 (1978).

6) S. Ooi, D. Carter, and Q. Fernando, *J. Chem. Soc., Chem. Commun.*, **1967**, 1301.

7) G. R. Desiraju, H. R. Luss, and D. L. Smith, *J. Am. Chem. Soc.*, **100**, 6375 (1978).

8) International Tables for X-ray Crystallography, (1974) Vol. IV, Birmingham, Kynoch Press.

9) M. C. Lim, E. Sinn, and R. B. Martin, *Inorg. Chem.*, **15**, 807 (1976).

10) O. P. Anderson, *J. Chem. Soc., Dalton Trans.*, **1973**, 1237.